RADIATIVE-TRANSFER MODEL REFLECTANCE SPECTRA OF POTENTIAL CERES MINERAL ASSEMBLAGES. David T. Blewett[1] and Connor L. Levy[2], [1]Johns Hopkins University Applied Physics Laboratory, Laurel, MD, 20723 USA (david.blewett@jhuapl.edu); [2]Century High School, Sykesville, MD 21784, USA (levyconnor@gmail.com).

Introduction: The *Dawn* spacecraft will rendezvous with the dwarf planet Ceres in 2015 [1]. The surface of Ceres is inferred to have a composition resembling that of carbonaceous chondrite meteorites [e.g., 2], quite different from the volcanic and plutonic rocks of *Dawn*'s first target, Vesta. Reflectance spectra of Ceres in the visible to near-infrared (NIR) wavelength range obtained with Earth-based telescopes are mostly featureless, although spectral features in the mid-infrared have been used to identify carbonates and alteration phases such as brucite (magnesium hydroxide, $Mg(OH)_2$) [3]. The *Dawn* Visible and InfraRed (VIR) [4] imaging spectrometer will measure the reflectance of the cerean surface from ~0.4 to 5.0 μm. The seven bandpass filters (0.438, 0.555, 0.653, 0.749, 0.829, 0.917, 0.965 μm) of *Dawn*'s multispectral Framing Cameras (FC) [5] are optimized for characterizing the mafic silicate mineral assemblages (basalts and orthopyroxenites) found on Vesta. During portions of the Ceres mission in low-altitude orbit, operational constraints may limit the FC to use of as few as three of the filters. Here we use Hapke's radiative transfer intimate mixing model [6] to predict spectra of assemblages of plausible Ceres minerals. We present FC spectral parameters and filter selections that may be most useful for mapping compositional differences on the cerean surface. Future studies will examine space weathering of Ceres analog assemblages.

Data and Model: We obtained laboratory reflectance spectra of analog minerals that are relevant to Ceres [3, 7] from the RELAB public database [8]. These include brucite, lizardite (a hydrous Mg-Fe phyllosillicate of the serpentine group), dolomite, magnesite, magnetite, and amorphous carbon, as well as the carbonaceous chondrite Murchison. We also examine the effects of water frost, which could be present at high latitudes on Ceres. Our Hapke spectral mixing model is adapted from one employed for a variety of lunar and meteoritic studies [9]. In Hapke's model, the reflectance spectrum of an intimate mixture depends on the single-scattering albedo of the individual constituents. To compute model reflectance spectra, we first converted the RELAB reflectance spectra to single-scattering albedo. The single-scattering albedo of water ice was calculated from published optical constants [10]. All model grain sizes were assumed to be 40 μm. The end-member reflectance spectra over the wavelength range 0.3 to 2.6 μm are shown in Fig. 1. Figures 2 and 3 present the brighter and darker spectra separately to allow more detail to be seen.

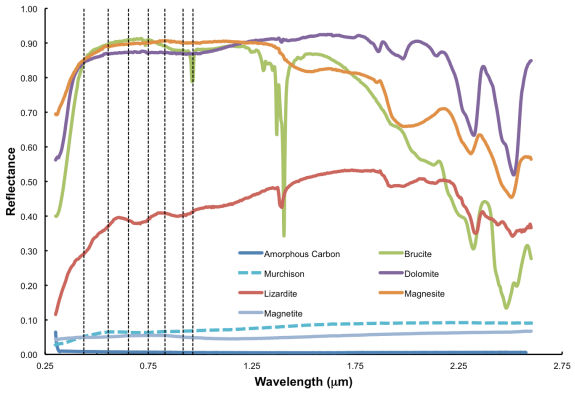

Figure 1. Laboratory reflectance spectra for Ceres analog minerals and for the Murchison carbonaceous chondrite meteorite. Vertical lines mark the center wavelengths of the seven FC filters.

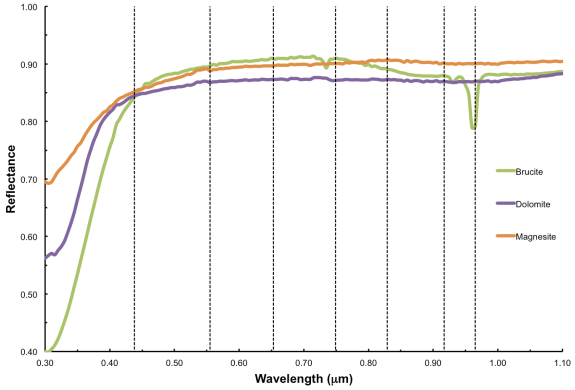

Figure 2. Laboratory reflectance spectra for the brighter Ceres analog minerals of Fig. 1 (0.3 to 1.1 μm). Vertical dashed lines mark the center wavelengths of the seven FC filters.

Discussion: Figure 4 presents four of our model mixture spectra along with a combined visible-IR telescopic spectrum of Ceres [11,12]. The mixture of 10% magnetite and 90% brucite is a moderately good fit to the Ceres telescopic spectrum, although the lizardite-containing assemblages are a better match to Ceres at wavelengths <0.55 μm. The addition of water frost to

the mixtures produces prominent absorptions near 1.5 and 2.0 μm.

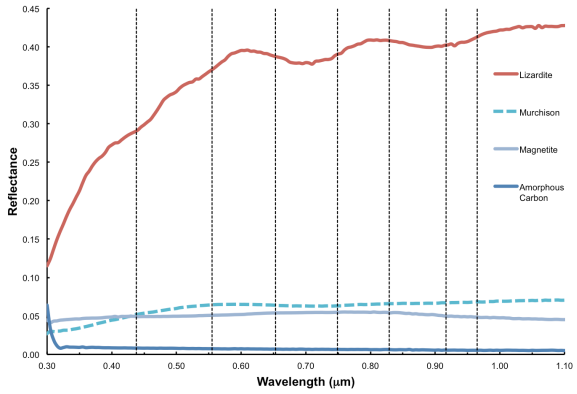

Figure 3. Laboratory reflectance spectra for the darker Ceres analog minerals of Fig. 1 (0.3 to 1.1 μm). Vertical dashed lines mark the center wavelengths of the seven FC filters.

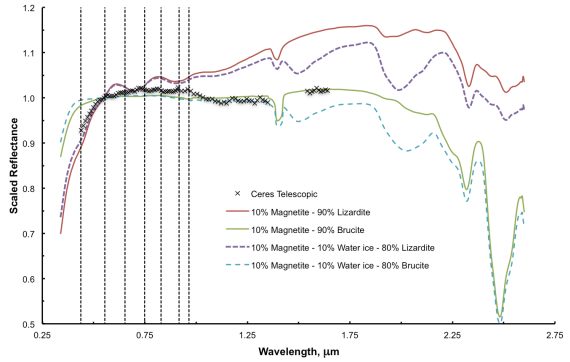

Figure 4. Model reflectance spectra for mixtures of analog minerals, plotted with a Ceres telescopic spectrum. Spectra are scaled to 1.0 at 0.55 μm.

To assess the ability of various FC filter combinations to discriminate among the analog minerals, we examined sets of reflectance ratios. Figure 5 is a plot of the 0.438-μm/0.829-μm reflectance ratio against the 0.965-μm/0.829 μm ratio for the spectra in Fig. 1. Use of the 0.965-μm band rather than 0.917-μm appears to better capture the depth of the OH absorption in lizardite. The 0.438-μm filter helps to measure the turndown toward the ultraviolet, and can separate brucite-dolomite-magnesite from lizardite (Figs. 4 and 5). Similar degrees of separation are achieved if the 0.555- or 0.749-μm filters are substituted for 0.829 μm in the ratios. Thus, if operational considerations limit imaging to three filters, we would recommend 0.438- and 0.965-μm, plus one of 0.555-, 0.749-, or 0.829-μm.

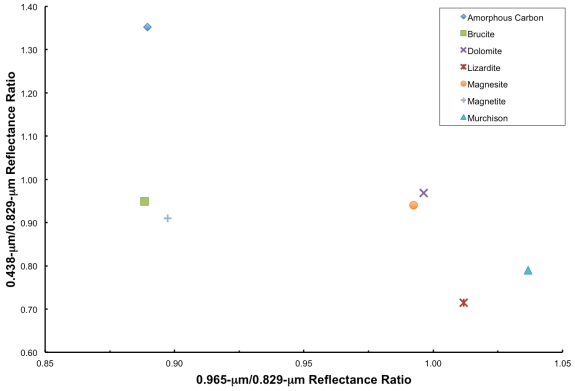

Figure 5. Spectral ratio plot for the analog spectra in Fig. 1. The 0.965-μm/0.829-μm reflectance ratio offers good dynamic range.

The effects of space weathering on asteroids are not well understood. Vesta appears to lack lunar-style optical alteration caused by accumulation of nanophase metallic iron (npFe^0) [13,14]. On the other hand, S-type asteroids do appear to undergo the reddening and diminution of mafic mineral bands that are associated with lunar-style space weathering [e.g., 15,16]. The surface of Ceres likely contains some iron-bearing phases (endogenic and/or exogenic) that could conceivably serve as the source of vapor-phase deposits of metallic iron produced during bombardment by micrometeoroids or solar-wind ions. We plan to perform additional radiative-transfer modeling that includes the effects of npFe^0 on the analog Ceres mineral assemblages. The space-weathering trends predicted by these model spectra can be compared to observations made by *Dawn* upon its arrival at Ceres.

References: [1] C.T. Russell et al. (2007), *Earth Moon Planets 101*, 65–91. [2] T.B. McCord et al. (2011), *Space Sci. Rev. 163*, 63–76. [3] R.E. Milliken and A.S. Rivkin (2009), *Nature Geosci. 2*, DOI: 10.1038/NGEO478. [4] M.C. De Sanctis et al. (2011), *Space Sci. Rev. 163*, 329–369. [5] H. Sierks et al. (2011), *Space Sci. Rev. 163*, 263–327. [6] B. Hapke (1981), *JGR 86*, 3039–3054. [7] A.S. Rivkin et al. (2011), *Space Sci. Rev. 163*, 95–116. [8] http://www.planetary.brown.edu/relab/ . [9] S.J. Lawrence and P.G. Lucey (2007), *JGR 112*, E07005. [10] S.G. Warren (1984) *Appl. Opt. 23,* 1206–1225. [11] S.J. Bus and R.P. Binzel (2002), *Icarus 158*, 106–145. [12] T.H. Burbine and R.P. Binzel (2002), *Icarus 159*, 468–499. [13] C.M. Pieters et al. (2012) *Nature 491*, 79–82. [14] D.T. Blewett et al. (2013), *LPS 44th* (this volume). [15] B. Hapke (2001), *JGR 106*, 10,039–10,073. [16] P. Vernazza et al. (2009), *Nature 458*, 993–995.